Am J Physiol Renal Physiol 293: F1157–F1165, 2007.
First published July 3, 2007; doi:10.1152/ajprenal.00411.2006.

Proteomic analysis defines altered cellular redox pathways and advanced glycation end-product metabolism in glomeruli of *db/db* diabetic mice

Michelle T. Barati,[1] Michael L. Merchant,[1,2] Angela B. Kain,[1,2] Anthony W. Jevans,[3] Kenneth R. McLeish,[1] and Jon B. Klein[1,2]

[1]*Department of Medicine and* [2]*Core Proteomics Laboratory, University of Louisville, and* [3]*Jewish Hospital and St. Mary Hospital, Louisville, Kentucky*

Submitted 18 October 2006; accepted in final form 28 June 2007

Barati MT, Merchant ML, Kain AB, Jevans AW, McLeish KR, Klein JB. Proteomic analysis defines altered cellular redox pathways and advanced glycation end-product metabolism in glomeruli of *db/db* diabetic mice. *Am J Physiol Renal Physiol* 293: F1157–F1165, 2007. First published July 3, 2007; doi:10.1152/ajprenal.00411.2006.—To attain a profile of protein expression during diabetes, we applied proteomic analysis to glomeruli of 160-day-old *db/db* diabetic and *db/m* nondiabetic mice. Glomerular proteins were extracted and separated by two-dimensional gel electrophoresis to construct a proteome map. Matrix-assisted laser desorption and ionization-time of flight mass spectrometry and peptide mass fingerprinting were used to identify 190 proteins. Of 105 analyzed spots, expression of 40 proteins, including the antioxidative enzymes peroxiredoxin 1 and 3, glutathione peroxidase 1, and SOD-1, was increased with diabetes, suggesting an adaptive response to oxidative stress associated with this diabetic model. However, activity of glutathione peroxidase and SOD was unaltered in glomeruli of diabetic mice. Expression of glyoxalase I was increased in glomeruli of diabetic mice. Because the cofactor for glyoxalase I, glutathione, is decreased in renal cortex of *db/db* mice, renal cortical glyoxalase I activity was measured in vitro with fixed amounts of exogenous glutathione. Glyoxalase I activity was decreased in renal cortex of *db/db* mice. These data indicate that diabetes-induced decreases in glyoxalase I activity are likely to be due to glutathione-dependent and -independent mechanisms and that increased expression of glyoxalase I may represent an insufficient adaptive response to increased methylglyoxal formation.

protein expression; glomeruli; glyoxalase I

DIABETIC NEPHROPATHY (DN) is the most common cause of chronic renal failure, accounting for nearly half of all new patients requiring dialysis, and is the leading cause of death among diabetic patients (46). Type 2 diabetes mellitus accounts for the majority of diabetic patients with nephropathy. The renal glomerulus is a major target of injury in DN and subject to capillary basement membrane thickening and expansion of the mesangium. Metabolic and hemodynamic disturbances associated with diabetes are clearly responsible for some of the glomerular pathology. The hemodynamic component is believed to be initiated by increased blood flow and pressure in the glomerular capillary bed, with the ensuing shear stress initiating a sclerotic response (11). High blood glucose concentrations result in increased influx of glucose into glomerular cells, leading to metabolic disturbances. Products of glucose metabolism by glycolysis, as well as the polyol pathway, ultimately result in formation of advanced glycation end products (AGE) and renal fibrosis (9). Cellular signaling pathways involving activation of protein kinases and transcription factors are also initiated by high glucose concentrations (37).

Despite our understanding of these hemodynamic and metabolic changes, the molecular mechanisms leading to DN are poorly defined. Functional genomic approaches have provided a valuable means of attaining a global view of the effect of diabetes on gene expression. Genomic profiling studies of kidney and glomeruli from diabetic mice, as well as mesangial cells propagated in high glucose, have identified differential expression of numerous genes (3, 10, 23, 24, 26–28, 40). Validation of these findings followed by analysis of protein expression of the respective genes may provide additional potential mechanisms involved in DN.

To attain an initial profile of protein expression in glomeruli during an overt stage of DN, we applied proteomic analysis to glomeruli of *db/db* diabetic and *db/m* nondiabetic mice. A total of 190 glomerular proteins were identified by matrix-assisted laser desorption and ionization-time of flight (MALDI-TOF) mass spectrometry (MS) and peptide mass fingerprinting. Expression of antioxidative enzymes and glyoxalase I was increased in glomeruli of diabetic mice. However, glyoxalase I activity was decreased in renal cortex of *db/db* mice. These results indicated a potential adaptive mechanism to diabetes-induced oxidative stress.

RESEARCH DESIGN AND METHODS

All studies on mice were approved by and conducted in accordance with the University of Louisville Institutional Animal Care and Use Committee guidelines. Female *db/db* and *db/m* mice on C57BLKS/J background were purchased from Jackson Laboratories (Bar Harbor, ME). Animals were maintained on a 12:12-h light-dark cycle at 25°C and given free access to water and food. Serum glucose was assayed on the Beckman Coulter DxC using glucose oxidase with an oxygen electrode.

Isolation of glomeruli. Mouse glomeruli were isolated according to the method described by Takemoto et al. (41). Briefly, 160-day-old mice were anesthetized with ketamine HCl-xylazine HCl; then the heart was perfused with a 30-ml suspension of 4.5-μm magnetic beads (Dynal, Lake Success, NY) in PBS, with the vena cava cut. The cortex of excised kidneys was dissected, minced with a razor blade, and subjected to digestion with type IA collagenase (1 mg/ml) for 30 min at 37°C. The suspension was gently pressed through a 100-μm cell strainer, and the filtrate was passed through an additional strainer. Glomeruli were isolated from the final filtrate with a magnetic particle concentrator (Dynal). The purity of isolated glomeruli was examined by visualization under a microscope.

Address for reprint requests and other correspondence: J. B. Klein, Kidney Disease Program, Univ. of Louisville, Baxter Biomedical Bldg 1, 570 S. Preston St., Louisville, KY 40202 (e-mail: Jon.klein@louisville.edu).

The costs of publication of this article were defrayed in part by the payment of page charges. The article must therefore be hereby marked "*advertisement*" in accordance with 18 U.S.C. Section 1734 solely to indicate this fact.

 0363-6127/07 $8.00 Copyright © 2007 the American Physiological Society

Glomerular protein extraction and separation by two-dimensional gel electrophoresis. Glomerular proteins were extracted by addition of buffer containing 7 M urea, 2 M thiourea, 65 mM 3-[(3-cholamidopropyl)dimethylammonio]-1-propanesulfonate, 58 mM DTT, and 4.5% ampholytes (pH 3–10) and then incubated for 1 h with constant stirring. Protein concentration of the soluble fraction was measured using the Bradford assay (Bio-Rad, Hercules, CA).

Immobilized pH gradient (IPG) strips (pH 3–10; Invitrogen, San Diego, CA) were rehydrated overnight with 75 μg of glomerular protein in rehydration buffer (Genomic Solutions, Ann Arbor, MI). Proteins were separated by isoelectric focusing using the ZOOM IPG Runner (Invitrogen) and then separated in the second dimension on 4–12% Bis-Tris gels, as described in detail previously (18). After electrophoresis, gels were fixed in 40% methanol-10% acetic acid solution for 30 min and stained with Sypro-Ruby protein stain (Bio-Rad) for 18 h.

Image acquisition and quantitative analysis of protein expression. Sypro-Ruby-stained two-dimensional (2-D) gels were scanned with a ProXPRESS fluoroimager (Perkin-Elmer, Boston, MA). Images were acquired at various exposure times to achieve equal and submaximal gray-level intensities for all gels.

Progenesis Discovery software (Non Linear Dynamics, Durham, NC) was used to match protein spots between gels and analyze the relative pixel intensity of protein spots. Spot pixel values were normalized to the gel total protein volume and subjected to background subtraction. Normalized intensity values of protein spots were used for comparison of protein expression between the two groups. Five different glomerular 2-D gels were analyzed from each group.

In-gel trypsin digestion, MALDI-TOF MS, and peptide mass fingerprinting. Protein spots were excised from gels and subjected to in-gel trypsin digestion (43). Trypsin-generated peptides were submitted for MALDI-TOF MS analysis as previously described (43). Mass spectral data were obtained using a Tof-Spec 2E (Micromass) and a 337-nm N_2 laser at 20–35% power in the reflector mode. Spectral data were obtained by averaging 10 spectra, each of which was the composite of 10 laser firings. Mass axis calibrations were accomplished using peaks from tryptic autohydrolysis. Peptide masses obtained by MALDI MS were analyzed using the Mascot search engine (www.matrixscience.com) by comparison with the SwissProt protein database. Search criteria included *Mus musculus* for taxonomy and allowing one missed cleavage for trypsin. Carbamidomethylation was chosen as a fixed modification and methionine oxidation as a variable modification. A maximal tolerance of 150 ppm was allowed for monoisotopic masses. A probability-based molecular weight search (MOWSE) score >74 indicated a significant match that was not a random event.

Western blotting. Glomerular proteins were extracted by lysis with 1% Triton X-100, 1% NP-40, 10% glycerol, 137 mM NaCl, 20 mM Tris·HCl, 1 ng/μl aprotinin, 1 ng/μl leupeptin, 4 mM PMSF, 20 mM NaF, and 1 mM Na_3VO_4. Samples were prepared by addition of Laemmli buffer and boiling for 5 min, followed by electrophoresis on 4–12% Bis-Tris gels. Proteins were electrophoretically transferred to PVDF membranes and immunoblotted using goat anti-PRX-3 or rabbit anti-SOD-1 (Santa Cruz Biotechnology, Santa Cruz, CA) antibodies in Odyssey infrared imaging blocking buffer (Licor, Lincoln, NE) supplemented with 0.1% Tween 20. Proteins were visualized by incubation of membranes with fluorescent-tagged anti-goat and anti-rabbit antibodies (Molecular Probes, Carlsbad, CA) and scanning on an Odyssey infrared imager (Licor).

Immunohistochemistry. Immunohistochemistry of paraffin-embedded kidney sections from 160-day-old *db/db* and *db/m* mice was performed as previously described (42) using rabbit anti-SOD-1 or goat anti-GPX-1 (Santa Cruz) at dilutions of 1:500 and 1:200, respectively.

Glyoxalase I activity assay. Cytosolic fractions of mouse renal cortical sections were prepared as previously described (39). The in vitro glyoxalase I activity assay was performed by addition of 20 μl of cytosolic fraction to reaction mixture containing 182 mM imidazole-HCl, 14.6 mM $MgSO_4$, 7.9 mM methylglyoxal (MG), and 1 mM glutathione, which had been equilibrated for 4 min before addition of sample (39). One unit of glyoxalase I activity was equivalent to the amount of enzyme required to form 1 μmol of *S*-D-lactoylglutathione per minute. Specific activity of glyoxalase I was then expressed as units of activity per milligram of total protein.

SOD and glutathione peroxidase activity assay. Activity of SOD and glutathione peroxidase (GPX) in renal cortex and glomeruli was determined using assay kits (catalog nos. 574601 and 353919, Calbiochem, San Diego, CA). For SOD, cytosolic fractions of cortex and glomeruli were prepared by homogenization in buffer containing 20 mM HEPES (pH 7.2), 1 mM EGTA, 210 mM mannitol, and 70 mM sucrose followed by centrifugation at 10,000 *g* for 15 min at 4°C. The SOD activity assay utilized reduction of a tetrazolium salt by xanthine oxidase-generated superoxide radicals. One unit of SOD activity is defined as the amount of enzyme required to exhibit 50% dismutation of superoxide radical. For GPX, tissue cytosolic fractions were prepared by homogenization in buffer containing 50 mM Tris·HCl (pH 7.5), 5 mM EDTA, and 1 mM DTT. Soluble proteins were collected by centrifugation as described above. The assay measures the decrease in absorbance at 340 nm resulting from oxidation of NADPH to $NADP^+$ by glutathione reductase in a coupled reaction to regenerate reduced glutathione consumed by GPX-mediated hydroperoxide reduction. One unit of activity is the amount of enzyme causing oxidation of 1 nmol of NADPH to $NADP^+$ per minute. For both assays, enzyme activity units were normalized to sample protein amount, which was divided by tissue expression ratio of the enzymes in *db/db* mice to that in *db/m* mice, which had been determined by proteomic analysis (for glomeruli) and Western blotting (for cortex).

Statistical analysis. Statistical analysis of relative spot pixel intensity from 2-D gels ($n = 5$ each group) and analysis of glyoxalase I, SOD, and GPX activity ($n = 4$ each group) were performed using two-tailed, unpaired *t*-test. $P < 0.05$ was considered significant.

RESULTS

Proteome map of mouse renal glomeruli. Renal glomeruli were isolated from 160-day-old *db/m* mice. Mice of this age were selected because age-matched *db/db* mice are well characterized to exhibit glomerular hypertrophy and expansion of the mesangium, as well as albuminuria, representative of overt DN (6, 38, 50). Serum glucose concentrations were consistently >550 mg/dl in diabetic mice. Soluble proteins extracted by lysis of glomeruli with a urea/thiourea-based buffer were used for 2-D gel electrophoresis (2-DE) to construct a reference proteome map of mouse glomeruli. This map was later used to analyze expression of proteins from age-matched *db/db* and *db/m* mice. Figure 1 represents the reference proteome map of the mouse glomeruli. Approximately 600 proteins were routinely visualized on glomerular 2-D gels. Of these, 241 spots were excised from gels and subjected to in-gel trypsin digestion and submitted for MALDI-TOF MS and subsequent identification by peptide mass fingerprinting. Tryptic digests were searched against the National Center for Biotechnology Information database using the Mascot search engine, and a significant MOWSE score, as well as close correlation of theoretical mass and isoelectric point (p*I*) of protein to location of protein spot on 2-D gels, verified positive identifications. Of the excised spots, a total of 173 spots representing 190 total proteins were identified. Of the 173 protein spots, 17 (*spots 9, 26, 33, 41, 43, 106, 112, 140, 141, 150, 161, 164, 166, 177, 178, 179*, and *182*) consisted of comigrated protein mixtures.

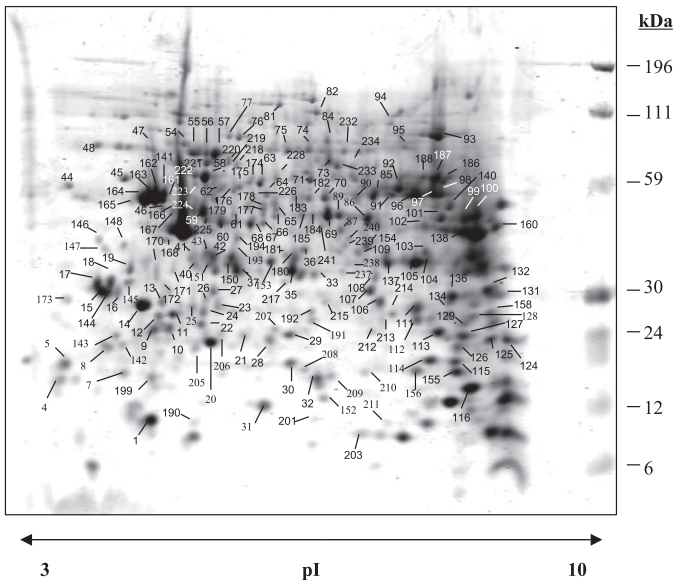

Fig. 1. Reference proteome map of *db/m* nondiabetic mouse renal glomeruli. Glomerular proteins were extracted by lysis with a urea/thiourea-based buffer, and soluble proteins were separated by 2-dimensional (2-D) gel electrophoresis (2-DE). Gels were stained with Sypro-Ruby fluorescent dye for visualization of proteins. Protein spots were excised, subjected to in-gel trypsin digestion, and identified by matrix-assisted laser desorption and ionization (MALDI)-time of flight mass spectrometry and peptide mass fingerprinting. A total of 190 proteins from 173 protein spots were identified from the map.

These comigrating spots were excluded from expression analysis.

Table 1 shows that 29 glomerular proteins were categorized as cytoskeletal and 13 as chaperones. Forty-two identified proteins were classified as participating in intermediary metabolism, including 11 glycolytic proteins, 13 proteins of the tricarboxylic acid cycle, and 18 proteins involved in the electron transport chain. Enzymes regulating cellular redox balance, ATP synthesis, and aldehyde metabolism comprised 15, 12, and 10 proteins, respectively. Fourteen proteins were classified as involved in cell metabolism, six in signal transduction, four in phospholipid binding and membrane fusion, and four in lipid homeostasis. Thirty-nine proteins were listed as miscellaneous, since no more than two proteins comprised a specific functional category. (For a complete list of identified proteins in each functional category, with corresponding gel spot number, theoretical mass and p*I*, SwissProt entry number, and expression with diabetes, see supplemental data for this article at the *American Journal of Physiology-Renal Physiology* website.)

Differential protein expression in glomeruli of db/db mice. To attain a profile of the long-term effects of diabetes on glomerular protein expression, protein spots on gels obtained from *db/db* and *db/m* mice were analyzed by spot matching and quantitation of relative pixel intensity of protein spots with use of Progenesis software. Expression of 105 protein spots was analyzed from 2-D gels, which included 16 unidentified protein spots. Expression analysis of the remaining 84 identified protein spots was impeded by overlap of protein spots in some regions of 2-D gels. Table 1 indicates the number of proteins in each functional group analyzed for expression. All glomerular proteins that exhibited a change in expression with diabetes were upregulated compared with glomeruli from nondiabetic mice. Expression of proteins within several functional categories was altered by diabetes. In the cytoskeletal category, expression of cofilin, gelsolin, tropomyosin, and vinculin was increased with diabetes. Genomic profiling of 5- to 7-wk-old *db/db* mice also showed increased gene expression of gelsolin. Expression of the glycolytic enzyme malate dehydrogenase was increased, whereas the cellular chaperones protein disulfide isomerase and glucose-regulated protein 78 were unaltered in glomeruli of diabetic mice. In addition to aldehyde reductase, expression of six proteins involved in maintaining cellular redox balance was increased by diabetes. Furthermore, expression of glyoxalase I was increased in glomeruli of diabetic mice. Similar to a previous report of increased gene expression in younger *db/db* mice (23), protein expression of carbonic anhydrase 2 was increased with diabetes.

The proteomic data were analyzed to determine how interrelated groups of proteins would be affected by diabetes-induced changes in protein expression. A prominent finding from the proteomic analysis was increased expression of glyoxalase I, inasmuch as this enzyme is critical to the metabolism of the AGE precursor MG. Glyoxalase I activity is significantly compromised during oxidative stress, which is known to occur in the diabetic kidney (30). Additionally, our proteomic analysis showed upregulation of five antioxidative enzymes with diabetes, suggesting an adaptive response to oxidative stress. Since diabetes is associated with increased oxidative stress and formation of AGEs, identification of altered expression of key enzymes involved in these pathways suggests an adaptive response to altered cellular function associated with diabetes.

Validation of increased expression of antioxidative enzymes in glomeruli of db/db mice. Expression analysis of glomerular proteins from *db/db* and *db/m* mice defined upregulation of antioxidative enzymes in diabetic mice. This group of proteins includes peroxiredoxin (PRX)-1, PRX-3, PRX-5, GPX-1, and SOD-1. Figure 2 demonstrates increased expression of SOD-1,

Table 1. *Classification of proteins identified from mouse glomerular proteome map*

Functional Group	No. of Proteins	No. of Proteins Analyzed for Expression	No. of Proteins Upregulated by Diabetes
Cytoskeletal	29	10	4
Chaperone	13	10	2
Glycolytic	11	3	1
TCA	13	7	2
Electron transport chain	18	9	2
Signaling	6	2	1
Ca^{2+} binding protein	2	1	0
Lipid homeostasis	4	3	1
Phospholipid binding	4	2	0
Reductive metabolism	15	8	6
ATPase	12	5	3
Aldehyde metabolism	10	4	2
General cell metabolism	14	8	2
Miscellaneous	39	17	6
Unidentified	16	16	8

TCA, tricarboxylic acid cycle. Normalized spot pixel intensity of each protein was averaged for the *db/m* and *db/db* groups and compared using 2-tailed, unpaired *t*-test ($n = 5$ in each group). $P < 0.05$ indicated significant regulation of protein expression with diabetes.

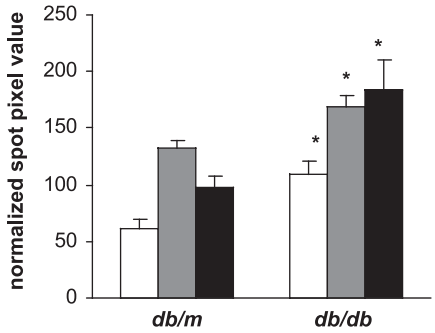

Fig. 2. Proteomic analysis reveals increased expression of antioxidative enzymes in glomeruli of *db/db* diabetic mice. Normalized protein spot pixel intensities from glomerular 2-D gels for SOD-1 (open bars), peroxiredoxin (PRX)-3 (shaded bars), and glutathione peroxidase (GPX)-1 (solid bars) are shown. Expression of SOD-1, PRX-3, and GPX-1 was increased by diabetes. Values are means ± SE ($n = 5$ in each group). *$P < 0.05$ vs. *db/m*.

PRX-3, and GPX-1 by 80, 28, and 90%, respectively, in glomeruli of diabetic mice. To validate results obtained by proteomic analysis, we analyzed expression of these three proteins by immunohistochemistry of kidney sections and Western blotting. Glomerular lysate from *db/m* and *db/db* mice was subjected to immunoblot analysis for PRX-3 and glyoxalase I. Figure 3 demonstrates increased expression of PRX-3 and glyoxalase I, respectively, in glomeruli of diabetic mice. Immunohistochemistry of kidney sections from 160-day-old mice from both groups revealed increased expression of SOD-1 in glomeruli of diabetic mice, especially in the peripheral region of the glomerular tuft, indicative of increased expression in the podocyte (Fig. 4*A*). The immunohistochemistry data also revealed decreased proximal tubular expression of SOD-1 in kidneys of *db/db* mice. This finding was further validated by an overall decreased expression of SOD-1 in renal cortex of *db/db* mice as determined by immunoblotting (Fig. 4*B*). Expression of GPX-1 was analyzed by immunohistochemistry as well. Figure 5 shows a global increase in glomerular GPX-1 expression in kidneys of *db/db* mice. Thus, findings from the proteomic analysis were confirmed for these antioxidative enzymes. The findings suggest an adaptive glomerular response to diabetes-induced oxidative stress that is absent in the renal tubule.

SOD and GPX activity in renal glomeruli and cortex of db/db and db/m mice. Previous studies reported alteration in activities of antioxidative enzymes in whole kidney and cortex during diabetes (13, 21). Inasmuch as activity of GPX and SOD is altered by nitration and MG (12, 17, 25, 32) and kidneys of *db/db* mice exhibit increased nitrotyrosine levels and AGEs, activity of these enzymes was analyzed in cytosolic fractions of glomeruli and cortex from both mouse groups. Renal cortical GPX-1 protein expression was analyzed by immunoblotting and found to be increased by 89% (Fig. 6*A*), as in the glomeruli. Activity of GPX was found to be unaltered by diabetes in glomeruli (Fig. 6*B*) and cortex (Fig. 6*C*). Glomerular SOD activity was unaltered (Fig. 7*A*), whereas cortical activity was increased (Fig. 7*B*), in *db/db* mice.

Decreased glyoxalase I activity in renal cortex of diabetic mice. Oxidative stress decreases reduced glutathione levels in the kidney during diabetes mellitus (30, 36). Because the activity of glyoxalase I is highly dependent on the availability of reduced glutathione, these findings suggested that glyoxalase I activity would be decreased in glomeruli of diabetic mice, despite an increase in expression of the enzyme. Renal cortex from *db/db* and *db/m* mice was used to analyze glyoxalase I activity. We first analyzed protein expression of glyoxalase I in renal cortex of mice in the two groups. As indicated in Fig. 8*A*, expression of glyoxalase I was 50% higher in renal cortex of *db/db* mice. Proteomic analysis of glomeruli determined that glyoxalase I protein expression was increased by 50% in *db/db* mice (Fig. 8*B*). Therefore, renal cortical glyoxalase I expression is increased to the same extent as in glomeruli. Glyoxalase I activity in cytosolic fractions of renal cortex from 160-day-old *db/db* and *db/m* mice was determined in an in vitro activity assay in which MG was used as substrate and reduced glutathione as cofactor. Activity of glyoxalase I was significantly decreased in the cortex of diabetic mice (Fig. 8*C*).

DISCUSSION

The renal glomerulus is a major target of injury in DN. The goal of the present study was to analyze global protein expression in the renal glomerulus during the overt stage of DN. The novel finding of the present study was upregulation in glomeruli from *db/db* mice of components within two divergent, yet interrelated, cellular pathways, the antioxidative system and the glyoxalase system. The lack of concurrent increase in GPX and SOD activity with increased protein expression in glomeruli of *db/db* mice suggests inactivation of these enzymes during diabetes. Furthermore, glyoxalase I activity was decreased in renal tissue from diabetic mice. Inasmuch as glyoxalase I activity is compromised during oxidative stress, the results suggest an inadequate adaptive mechanism by glomeruli, resulting in impaired MG metabolism during diabetes.

We used proteomic analysis to attain a profile of protein expression in glomeruli of the *db/db* mouse model of type 2 diabetes mellitus. The *db/db* mouse is a well-characterized model of diabetic kidney disease exhibiting such features as renal and glomerular hypertrophy, albuminuria, and expansion of the mesangium. This model has limitations, in that it does not exhibit the characteristic tubulointerstitial lesions and arteriolar hyalinosis observed in human DN (38). The mechanisms underlying glomerular pathologies in the *db/db* mouse are not completely defined.

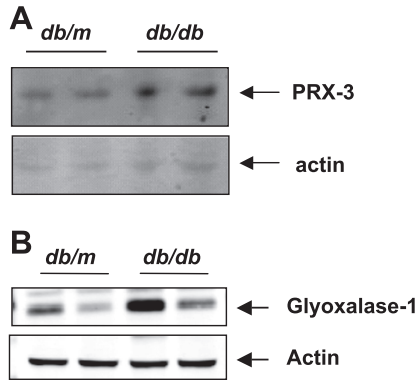

Fig. 3. Increased expression of PRX-3 and glyoxalase I in glomeruli of *db/db* mice. Expression of PRX-3 and glyoxalase I in glomeruli of *db/db* and *db/m* mice was analyzed by immunoblot analysis. Each lane represents extracts from independent mouse glomeruli. Blots were reprobed for β-actin to demonstrate equal loading of protein between lanes.

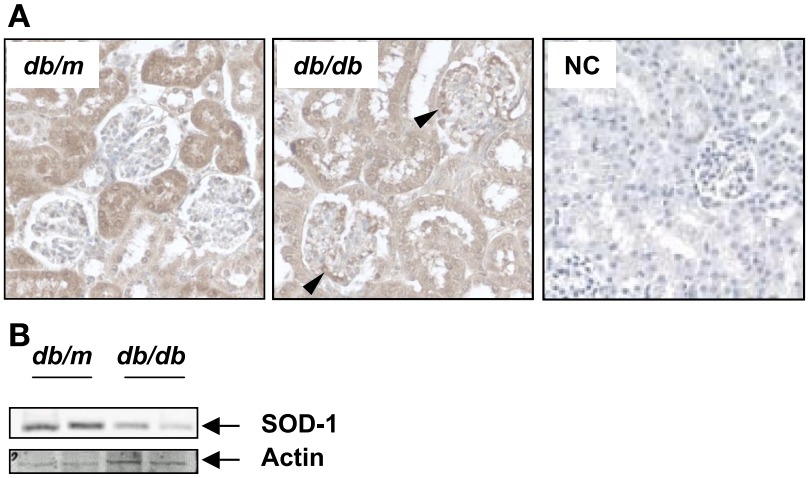

Fig. 4. Immunohistochemical staining of *db/db* and *db/m* mouse kidney sections for SOD-1 confirms increased glomerular expression with diabetes. *A*: SOD-1 expression was increased in glomeruli and decreased in tubules of *db/db* mice. Arrowheads indicate increased staining in podocytes. Negative control for staining (NC) was performed by incubation of kidney sections with nonimmune antibodies, and nuclei were stained with hematoxylin. Magnification ×40. *B*: immunoblot of renal cortex for SOD-1 indicates decreased expression with diabetes. Blot was reprobed for β-actin to demonstrate equal loading of protein between lanes.

The proteomic analysis used in this study served two purposes. *1*) By separating glomerular proteins by 2-DE, we were able to construct a proteome map and database of mouse glomerular proteins. *2*) 2-D separation and staining of proteins allowed quantitation of individual protein spot pixel intensity, which was used as a measure of expression level for each protein. Of the ~600 visible protein spots, 190 proteins, comprising multiple cellular functional categories, were identified. These data represent an initial effort to construct a murine glomerular protein database, which can be used for subsequent studies. The data presented here support and extend a human glomerular proteomic map recently reported by Yoshida et al. (53) in which 347 proteins from human glomeruli were identified by MALDI-MS and peptide mass fingerprinting and liquid chromatography-tandem MS. However, in this report, we have concentrated our efforts on identifying proteins that were differentially expressed between *db/db* and *db/m* mice.

To identify proteins regulated in diabetes, we compared expression of glomerular proteins from *db/db* and *db/m* mice separated by 2-DE. Of the 105 protein spots analyzed for expression, 40 were found to be upregulated in glomeruli of diabetic mice. The present study is the first to analyze global protein expression changes in glomeruli with diabetes. Genomic expression profiling of glomeruli from 5- to 7-wk-old (23) and 13-wk-old (27) *db/db* mice has identified 116 and 779 differentially regulated genes, and 343 genes of kidneys from 150-day-old *db/db* mice were regulated (40). In addition, renal cortex from *db/db* mice demonstrates differential expression of genes during initial and overt phases of DN (24). The increased number of regulated gene products in these studies may reflect the generally acknowledged superior sensitivity of mRNA assays to protein methods. This is demonstrated by the presence of ~15% of proteins expected to be expressed in cells visualized on 2-D gels in the present study. The low representation of the tissue's proteome on 2-D gels is a result of omission of proteins, such as membrane proteins, with the extraction procedures utilized, as well as masking of low abundant proteins due to poor resolution of proteins separated with p*I* in the range of 3–10, for densitometric/expression analysis. Additionally, a number of spots from the 2-D gel were analyzed by MALDI-MS without adequate spectra for identification. This may be due to incomplete trypsin digestion of excised gel pieces or incomplete extraction of trypsin-digested peptides from Bis-Tris gels. Inasmuch as ~5,000–22,000 probes are used on gene array chips employed in genomic profiling studies of glomeruli and kidneys, the probability for identification of regulated products significantly increases. Genes for six of the proteins identified from the glomerular proteome map in the present study have been shown to be upregulated in 7-wk-old *db/db* mice (23), and a separate study found upregulation of genes for an additional six

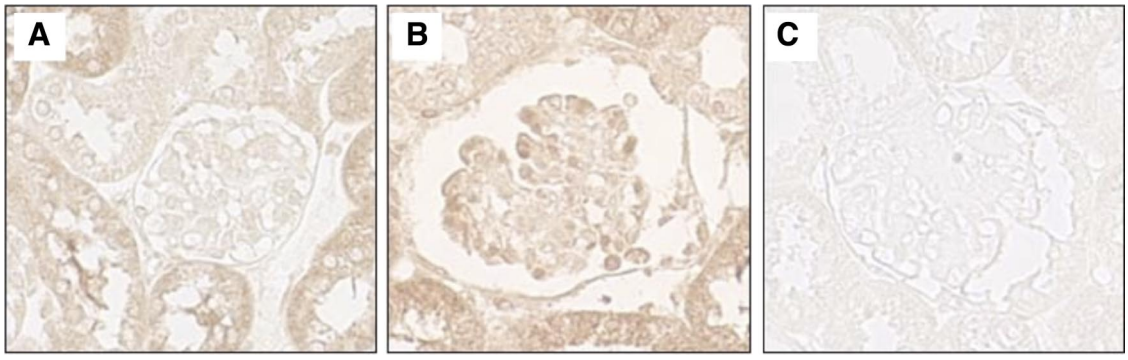

Fig. 5. Immunohistochemistry of kidney sections for GPX-1 confirms increased glomerular expression with diabetes. *A*: positive glomerular staining of GPX-1 was detected in kidney sections from *db/m* mice. *B*: GPX-1 expression was globally increased in glomeruli of *db/db* mice. *C*: negative control for staining was performed by incubation of kidney sections with nonimmune antibodies. No nuclear staining was performed. Magnification ×40.

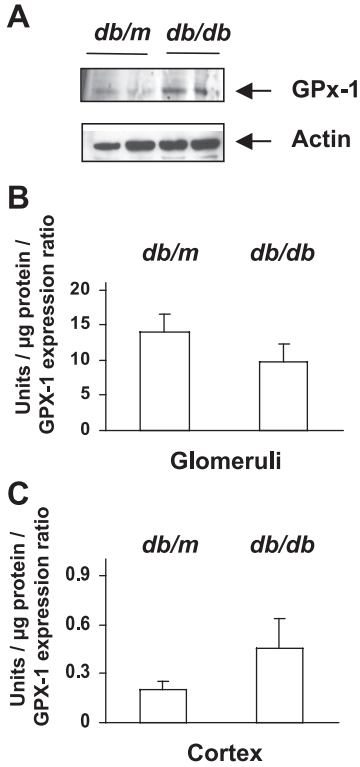

Fig. 6. GPX activity is unaltered in renal glomeruli and cortex of diabetic mice. *A*: renal cortex of *db/db* and *db/m* mice was analyzed for GPX-1 expression by immunoblotting. GPX-1 expression was increased by 89% in renal cortex of *db/db* mice ($n = 2$ in each group). Blot was reprobed for β-actin to demonstrate relative loading of protein between lanes. *B* and *C*: tissue GPX-1 activity was determined from the slope of the decrease in absorbance at 340 nm resulting from oxidation of NADPH to $NADP^+$ in a glutathione reductase-coupled reaction and the extinction coefficient for NADPH. Activity units ($nmol \cdot min^{-1} \cdot ml^{-1}$) were normalized to the amount of protein in the reaction and tissue expression ratio of the enzyme in *db/db* mice to that in *db/m* mice. GPX activity was unaltered in glomeruli and cortex of *db/db* mice. Values are means ± SE ($n = 4$ in each group for each tissue).

identified in the proteome in 13-wk-old *db/db* mice (27). Although concurrent reports for gene expressions of these 12 proteins in this age group are not known, protein expression of 3 of the proteins is upregulated in *db/db* mice used in the present study. Considered together, these studies clearly indicate the significance of understanding the temporal regulation of genes, their protein products, and the resulting interrelation of the protein products in regulating cellular signaling pathways responsible for the pathogenesis of DN.

One advantage of proteomic analysis of glomeruli obtained from animal models of diabetes is that cellular activities may be predicted from expression profiles of groups of proteins. Two prominent findings from our proteomic analysis were diabetes-induced upregulation of antioxidative enzymes and an enzyme of the glyoxalase system. The proteomic findings were validated for three of the upregulated antioxidative enzymes by immunoblotting of glomerular proteins for PRX-3 and immunohistochemistry of mouse kidney sections for GPX-1 and SOD-1. Peroxiredoxins reduce hydrogen peroxide and are distributed in the cytosol, mitochondria, peroxisomes, and plasma (15). GPX-1 is widely expressed throughout different tissues and reduces hydrogen peroxide by use of reduced glutathione, as well as lipid peroxides, in membranes (25). Immunohistochemistry of kidney sections for SOD-1 revealed increased expression in glomerular podocytes during diabetes. Additionally, SOD-1 expression was found to decrease in proximal tubule cells of *db/db* mice. Thus different adaptive responses may occur in the two different renal compartments. Nonetheless, these data indicate the importance of independent proteomic analysis of different renal compartments to define their contribution to the pathologies of DN. Previous studies on 150-day-old *db/db* mice report that renal cortical GPX activity increases while activity of SOD-1, SOD-2, and catalase remains unaltered (13). Glomerular gene expression of PRX-1, GPX-3, SOD-1, and catalase is increased in 7-wk-old *db/db* mice (23). In the KKAy mouse model of insulin-resistant diabetes, kidney GPX-1 and SOD-1 mRNA expression increases (16). Increased mRNA and activity of SOD-1 and GPX have also been reported in kidneys of streptozotocin (STZ)-induced diabetic rats after 6 wk (21), whereas glomerular transcript levels of these enzymes are unaltered (20) or increased (26) after 2 and 1 wk, respectively, in the same diabetic model. Glomerular protein expression of GPX has been shown to gradually decrease with duration of diabetes in STZ-induced diabetic rats (8). This is the first report of increased glomerular protein expression of several of these enzymes, including PRX-1 and PRX-5, in the *db/db* mouse model. The lack of parallel increase in GPX activity with increased GPX-1 protein expression in glomeruli and cortex and glomerular SOD activity in the present study may be due to inactivation of the enzymes by nitration (12, 25), as well as direct binding and inactivation by MG (32, 17), factors known to be increased in the kidney during diabetes. Additionally, alternative isozymes, such as extracellular GPX and SOD, may be differentially expressed and regulated by diabetes and present in the tissue homogenates used for the assays. The increase in cortical SOD

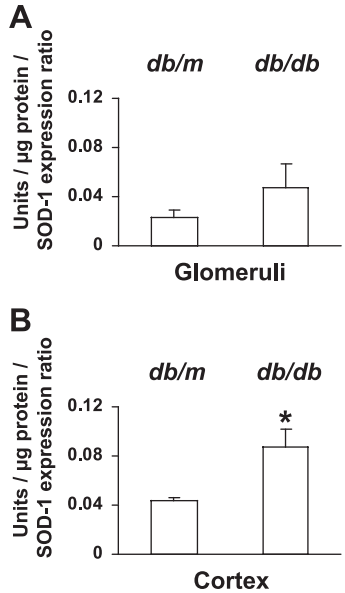

Fig. 7. SOD activity is unaltered in glomeruli and increased in renal cortex of diabetic mice. One unit of activity is equal to the amount of enzyme required to exhibit 50% dismutation of superoxide radical. Activity (units/ml) was normalized to the amount of protein in the reaction and tissue expression ratio of the enzyme in *db/db* mice to that in *db/m* mice. SOD activity was unaltered in glomeruli and increased in cortex of *db/db* mice. Values are means ± SE ($n = 4$ in each group for each tissue). *$P < 0.05$ vs. *db/m*.

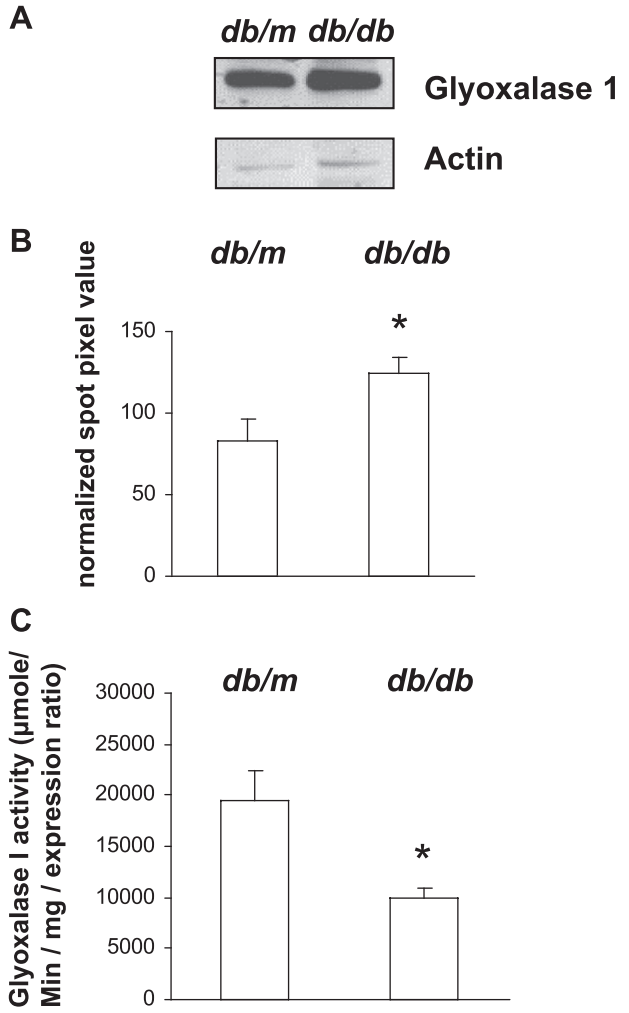

Fig. 8. Glyoxalase I activity is decreased in renal cortex of diabetic mice. *A*: renal cortex of *db/db* and *db/m* mice was analyzed for glyoxalase I expression by immunoblotting. Glyoxalase I expression was increased by 60% in renal cortex of *db/db* mice ($n = 3$ in each group). Blot was reprobed for β-actin to demonstrate equal loading of protein between lanes. *B*: analysis of protein spot pixel intensity of glomerular 2-D gels from *db/db* and *db/m* mice indicates a 50% increase in glyoxalase I expression with diabetes ($n = 5$ in each group). *C*: *db/db* and *db/m* mouse renal cortical glyoxalase I activity was determined in an in vitro assay of cytosolic fractions with reaction buffer containing methylglyoxal and glutathione as substrate and cofactor, respectively. Production of the resultant product, *S*-D-lactoylglutathione, was recorded by increased absorbance at 240 nm for 2 min. Glyoxalase I activity was determined from the linear portion of the reaction curve and normalized to total cytosolic fraction protein and then to cortical expression ratio of glyoxalase I in *db/db* mice to that in *db/m* mice. Glyoxalase I activity was decreased in renal cortex of *db/db* mice. Values are means ± SE [$n = 5$ (*B*) and 4 (*C*) in each group]. *$P < 0.05$ vs. *db/m*.

activity with concurrent decrease in SOD-1 protein expression may again reflect upregulated activity in alternate tissue types in cortex, such as vascular cells, and suggests that different renal cells may be differentially predisposed to hyperglycemia-induced perturbations. Evidence of renal oxidative stress in *db/db* mice has been shown previously in reports of increased kidney lipid peroxidation (22), nitrotyrosine expression (13), and decreased glutathione levels in renal cortex (13). In addition, treatment of *db/db* mice with astaxanthine, which exhibits antioxidant activity, significantly reduced the diabetes-induced increase in mesangial area and urinary albumin (27). Considered together, these reports and our data indicate an adaptive renal response to increased oxidative stress occurs in diabetes.

The glyoxalase system includes glyoxalase I and II and is critical in detoxification of cellular α-ketoaldehydes, such as MG (44, 35). MG is a highly reactive α-dicarbonyl produced as a metabolic product of glycolysis (31), as well as lipolysis (7), and is a precursor of AGEs. Type 1 and 2 diabetes is associated with increased MG levels, and subjects with more rapid progression of DN exhibit even higher MG production (4, 5). Therefore, the finding by the proteomic analysis of increased glyoxalase I expression seemed paradoxical, inasmuch as diabetes is known to be associated with increased formation of AGEs. However, other cellular mechanisms in addition to the glyoxalase system metabolize MG, including aldose reductase, aldehyde dehydrogenase 9, and 2-oxoaldehyde dehydrogenase (47, 52). Of these enzymes, glyoxalase I activity is ~10–40 times higher in most tissues of the body and is heavily compromised during oxidative stress, because it requires reduced glutathione as a cofactor (45). Glutathione is the most abundant intracellular thiol-based antioxidant; it functions as a sulfhydryl buffer and in detoxification of compounds by direct binding or conjugation via glutathione *S*-transferase (GST) (34). However, MG reacts with and inactivates glutathione reductase (48), leading to decreased availability of reduced glutathione and, hence, increased oxidative stress. Availability of reduced glutathione is further compromised by cellular enzymes, such as aldose and aldehyde reductases, competing with glutathione reductase for the cofactor NADPH. In the present study, proteomic analysis revealed increased expression of aldehyde reductase and one isoform of GST (GST-μ) in glomeruli of diabetic mice. Therefore, *db/db* mice exhibit upregulation of systems requiring the reduced form of glutathione (glyoxalase I and glutathione peroxidase) and NADPH (aldehyde reductase) and mechanisms to decrease total glutathione levels (GST-μ).

These results suggest that in situ glyoxalase I activity would be decreased in glomeruli of *db/db* mice, despite an increase in glyoxalase I protein expression due to decreased glutathione levels. Previous studies have found glyoxalase I activity to be unaltered in renal cortex, decreased in liver, and increased in muscle of STZ-induced diabetic rats (33). Additionally, erythrocytes of STZ-induced and *ob/ob* diabetic mice exhibit decreased glyoxalase activity (2). We measured in vitro glyoxalase I activity in cytosolic fractions of renal cortex from the two mouse groups and found it to be lower in *db/db* mice. Since the in vitro activity assays were performed in the presence of an equal catalytic amount of reduced glutathione, the results indicate that the diabetes-induced decrease in activity is likely to be glutathione dependent and independent. The glutathione-independent mechanisms may result from posttranslational modification of glyoxalase I in diabetes. In fact, PKA-mediated phosphorylation of glyoxalase I results in decreased enzymatic activity (49). Inasmuch as activity of several kinases, such as the mitogen-activated protein kinases (1), PKC (19), and Akt (14), is known to be increased in kidneys of *db/db* mice and PKA activity is increased in kidneys of STZ-induced diabetic rats (51), phosphorylation by any of these pathways may be responsible for decreased glyoxalase I activity in renal cortex of *db/db* mice. Decreased glyoxalase I activity in the kidney during diabetes may contribute significantly to cellular levels of MG and, ultimately, production of AGEs.

In summary, we report the construction of a 2-D proteome map of renal glomeruli of *db/db* mice that can be utilized as a comprehensive database for analysis of protein expression during experimental conditions. Proteomic analysis of glomerular proteins separated by 2-DE revealed upregulation of enzymes involved in cellular redox regulation and the glyoxalase system. These two divergent cellular pathways are interrelated by their effect on and need for reduced glutathione. Increased expression of enzymes in these two pathways may represent an insufficient adaptive response to the metabolic disturbances in diabetes.

GRANTS

This research was supported by National Institute of Diabetes and Digestive and Kidney Diseases Grant R21 DK-629086-01 (J. B. Klein), the Kentucky Research Challenge Trust, and an American Heart Association Ohio Valley Affiliate postdoctoral fellowship grant (M. T. Barati).

REFERENCES

1. **Adhikary L, Chow F, Nikolic-Paterson DJ, Stambe C, Dowling J, Atkins RC, Tesch GH.** Abnormal p38 mitogen-activated protein kinase signalling in human and experimental diabetic nephropathy. *Diabetologia* 47: 1210–1222, 2004.
2. **Atkins TW, Thonalley PJ.** Erythrocyte glyoxalase activity in genetically obese (*ob/ob*) and streptozotocin diabetic mice. *Diabetes Res* 11: 125–129, 1989.
3. **Baelde HJ, Eikmans M, Doran PP, Lappin DWP, de Heer E, Brujin JA.** Gene expression profiling in glomeruli from human kidneys with diabetic nephropathy. *Am J Kidney Dis* 43: 636–650, 2004.
4. **Beisswenger PJ, Howell SK, Nelson RG, Mauer M, Szwergold BS.** α-Oxoaldehyde metabolism and diabetic complications. *Biochem Soc Trans* 31: 1358–1363, 2003.
5. **Beisswenger PJ, Makita Z, Curphey TJ, Moore LL, Jean S, Brinck-Johnsen T, Bucala R, Vlassara H.** Formation of immunochemical advanced glycosylation end products precedes and correlates with early manifestations of renal and retinal disease in diabetes. *Diabetes* 44: 824–829, 1995.
6. **Breyer MD, Bottinger E, Brosius FC 3rd, Coffman TM, Harris RC, Heilig CW, Sharma K.** Mouse models of diabetic nephropathy. *J Am Soc Nephrol* 16: 27–45, 2005.
7. **Casazza JP, Felver ME, Veech RL.** The metabolism of acetone in rat. *J Biol Chem* 259: 231–236, 1984.
8. **Chiu YW, Kuo MC, Kuo HT, Chang JM, Guh JY, Lai YH, Chen HC.** Alterations of glomerular and extracellular levels of glutathione peroxidase in patients and experimental rats with diabetic nephropathy. *J Lab Clin Med* 145: 181–186, 2005.
9. **Chung SS, Ho EC, Lam KS, Chung SK.** Contribution of polyol pathway to diabetes-induced oxidative stress. *J Am Soc Nephrol* 14 *Suppl* 3: S233–S236, 2003.
10. **Clarkson MR, Murphy M, Gupta S, Lambe T, Mackenzie HS, Godson C, Martin F, Grady HR.** High glucose-altered gene expression in mesangial cells. Actin-regulatory protein gene expression is triggered by oxidative stress and cytoskeletal disassembly. *J Biol Chem* 277: 9707–9712, 2002.
11. **Cooper ME.** Interaction of metabolic and haemodynamic factors in mediating experimental diabetic nephropathy. *Diabetologia* 44: 1957–1972, 2001.
12. **Demicheli V, Quijano C, Alvarez B, Radi R.** Inactivation and nitration of human superoxide dismutase (SOD) by fluxes of nitric oxide and superoxide. *Free Radic Biol Med* 42: 1359–1368, 2007.
13. **DeRubertis FR, Craven PA, Melhem MF, Salah EM.** Attenuation of renal injury in *db/db* mice overexpressing superoxide dismutase: evidence for reduced superoxide-nitric oxide interaction. *Diabetes* 53: 762–768, 2004.
14. **Feliers D, Duraisamy S, Faulkner JL, Duch J, Lee AV, Abboud HE, Choudhury GG, Kasinath BS.** Activation of renal signaling pathways in *db/db* mice with type 2 diabetes. *Kidney Int* 60: 495–504, 2001.
15. **Fujii J, Ikeda Y.** Advances in our understanding of peroxiredoxin, a multifunctional, mammalian redox protein. *Redox Rep* 7: 123–130, 2002.
16. **Fujita A, Sasaki H, Ogawa K, Okamoto K, Matsuno S, Matsumoto E, Furuta H, Nishi M, Nakao T, Tsuno T, Taniguchi H, Nanjo K.** Increased gene expression of antioxidant enzymes in KKAy diabetic mice but not in STZ diabetic mice. *Diabetes Res Clin Pract* 69: 113–119, 2005.
17. **Kang JH.** Modification and inactivation of human Cu, Zn-superoxide dismutase by methylglyoxal. *Mol Cell* 15: 194–199, 2003.
18. **Klein JB, Barati MT, Wu R, Gozal D, Sachleben LR, Kausar H, Trent JO, Gozal E, Rane MJ.** Akt-mediated VCP phosphorylation regulates its association with ubiquitinated proteins. *J Biol Chem* 280: 31870–31881, 2005.
19. **Koya D, Haneda M, Nakagawa H, Isshiki K, Sato H, Maeda S, Sugimoto T, Yasuda H, Kashiwagi A, Ways DK, King GL, Kikkawa R.** Amelioration of accelerated diabetic mesangial expansion by treatment with a PKC-β inhibitor in diabetic *db/db* mice, a rodent model for type 2 diabetes. *FASEB J* 14: 439–447, 2000.
20. **Koya D, Hayashi K, Kitada M, Kashiwagi A, Kikkawa R, Haneda M.** Effects of antioxidants in diabetes-induced oxidative stress in the glomeruli of diabetic rats. *J Am Soc Nephrol* 14 *Suppl* 3: S250–S253, 2003.
21. **Limaye PV, Raghuram N, Sivakami S.** Oxidative stress and gene expression of antioxidant enzymes in the renal cortex of streptozotocin-induced diabetic rats. *Mol Cell Biochem* 243: 147–152, 2003.
22. **Lubec B, Hermon M, Hoeger H, Lubec G.** Aromatic hydroxylation in animal models of diabetes mellitus. *FASEB J* 12: 1581–1587, 1998.
23. **Makino H, Miyamoto Y, Sawai K, Mori K, Mukoyama M, Nakao K, Yoshimasa Y, Suga S.** Altered gene expression related to glomerulogenesis and podocyte structure in early diabetic nephropathy of *db/db* mice and its restoration by pioglitazone. *Diabetes* 55: 2747–2756, 2006.
24. **Mishra R, Emancipator SN, Miller C, Kern T, Simonoson MS.** Adipose differentiation-related protein and regulators of lipid homeostasis identified by gene expression profiling in the murine *db/db* diabetic kidney. *Am J Physiol Renal Physiol* 286: F913–F921, 2004.
25. **Miyamoto Y, Koh YH, Park YS, Fujiwara N, Sakiyama H, Misonou Y, Ookawara T, Suzuki K, Honke K, Taniguchi N.** Oxidative stress caused by inactivation of glutathione peroxidase and adaptive responses. *Biol Chem* 384: 567–574, 2003.
26. **Morrison J, Knoll K, Hessner MJ, Liang M.** Effect of high glucose on gene expression in mesangial cells: upregulation of the thiol pathway is an adaptational response. *Physiol Genomics* 17: 271–282, 2004.
27. **Naito Y, Uchiyama K, Mizushima K, Kuroda M, Akagiri S, Takagi T, Handa O, Kokura S, Yoshida N, Ichikawa H, Takahashi J, Yoshikawa T.** Microarray profiling of gene expression patterns in glomerular cells of astaxanthin-treated diabetic mice: a nutrigenomic approach. *Int J Mol Med* 18: 685–695, 2006.
28. **Naito Y, Uchiyama K, Kuroda M, Mizushima K, Aoi W, Kokura S, Ichikawa H, Yoshida N, Yoshikawa T.** Laser capture microdissection/GeneChip analysis of gene expression in glomerular cells in diabetic *db/db* mice. *Redox Rep* 9: 307–312, 2004.
29. **Naito Y, Uchiyama K, Aoi W, Hasegawa G, Nakamura N, Yoshida N, Maoka T, Takahashi J, Yoshikawa T.** Prevention of diabetic nephropathy by treatment with astaxanthin in diabetic *db/db* mice. *Biofactors* 20: 49–59, 2004.
30. **Obrosova IG, Fathallah L, Liu E, Nourooz-Zadeh J.** Early oxidative stress in the diabetic kidney: effect of DL-α-lipoic acid. *Free Radic Biol Med* 34: 186–195, 2003.
31. **Ohmori S, Mori M, Shiraha K, Kawase M.** Biosynthesis and degradation of methylglyoxal in animals. *Prog Clin Biol Res* 290: 397–412, 1989.
32. **Park YS, Koh YH, Takahashi M, Miyamoto Y, Suzuki K, Dohmae N, Takio K, Honke K, Taniguchi N.** Identification of the binding site of methylglyoxal on glutathione peroxidase: methylglyoxal inhibits glutathione peroxidase activity via binding to glutathione binding sites Arg 184 and 185. *Free Radic Res* 37: 205–211, 2003.
33. **Phillips SA, Mirrlees D, Thornalley PJ.** Modification of the glyoxalase system in streptozotocin-induced diabetic rats. Effect of the aldose reductase inhibitor Statil. *Biochem Pharmacol* 46: 805–811, 1993.
34. **Pompella A, Visvikis A, paolicchi A, De Tata V, Casini AF.** The changing faces of glutathione, a cellular protagonist. *Biochem Pharmacol* 66: 1499–1503, 2003.
35. **Ranganathan S, Walsh ES, Godwin AK, Tew KD.** Cloning and characterization of human colon glyoxalase-I. *J Biol Chem* 268: 5661–5667, 1993.
36. **Satoh M, Fujimoto S, Haruna Y, Arakawa S, Horike H, Komai N, Sasaki T, Tsujioka K, Makino H, Kashihara N.** NAD(P)H oxidase and uncoupled nitric oxide synthase are major sources of glomerular superoxide in rats with experimental diabetic nephropathy. *Am J Physiol Renal Physiol* 288: F1144–F1152, 2005.

37. **Schena FP, Gesualdo L.** Pathogenetic mechanisms of diabetic nephropathy. *J Am Soc Nephrol* 16 *Suppl* 1: S30–S33, 2005.
38. **Sharma K, McCue P, Dunn SR.** Diabetic kidney disease in the *db/db* mouse. *Am J Physiol Renal Physiol* 284: F1138–F1144, 2003.
39. **Shinohara M, Thornalley PJ, Giardino I, Beisswenger P, Thorpe SR, Onorato J, Brownlee M.** Overexpression of glyoxalase-I in bovine endothelial cells inhibits intracellular advanced glycation end product formation and prevents hyperglycemia-induced increases in macromolecular endocytosis. *J Clin Invest* 101: 1142–1147, 1998.
40. **Susztak K, Bottinger E, Novetsky A, Liang D, Zhu Y, Ciccone E, Wu D, Dunn S, McCue P, Sharma K.** Molecular profiling of diabetic mouse kidney reveals novel genes linked to glomerular disease. *Diabetes* 53: 784–794, 2004.
41. **Takemoto M, Asker N, Gerhardt H, Lundkvist A, Johansson BR, Saito Y, Betsholtz C.** A new method for large scale isolation of kidney glomeruli from mice. *Am J Pathol* 161: 799–805, 2002.
42. **Thongboonkerd V, Barati MT, McLeish KR, Benarafa C, Remold-O'Donnell E, Zheng S, Rovin BH, Pierce WM, Epstein PN, Klein JB.** Alterations in the renal elastin-elastase system in type 1 diabetic nephropathy identified by proteomic analysis. *J Am Soc Nephrol* 15: 650–662, 2004.
43. **Thongboonkerd V, Luengpailin J, Cao J, Pierce WM, Cai J, Klein JB, Doyle RJ.** Fluoride exposure attenuates expression of *Streptococcus pyogenes* virulence factors. *J Biol Chem* 277: 16599–16605, 2002.
44. **Thornalley PJ.** Glyoxalase I structure, function, and a critical role in the enzymatic defence against glycation. *Biochem Soc Trans* 31: 1343–1348, 2003.
45. **Thornalley PJ.** Pharmacology of methylglyoxal: formation, modification of proteins and nucleic acids, and enzymatic detoxification—a role in pathogenesis and antiproliferative chemotherapy. *Gen Pharmacol* 27: 565–573, 1996.
46. **US Renal Data System.** *US RDS 2004 Annual Data Report*. Bethesda, MD: National Institutes of Health, National Institute of Diabetes and Digestive and Kidney Diseases, 2004.
47. **Vander Jagt DL, Hunsaker LA.** Methylglyoxal metabolism and diabetic complications: roles of aldose reductase, glyoxalase-I, betaine aldehyde dehydrogenase and 2-oxoaldehyde dehydrogenase. *Chem Biol Interact* 143–144: 341–351, 2003.
48. **Vander Jagt DL, Hunsaker LA, Vander Jagt TJ, Gomez MS, Gonzales DM, Deck LM, Royer RE.** Inactivation of glutathione reductase by 4-hydroxynonenal and other endogenous aldehydes. *Biochem Pharmacol* 53: 1133–1140, 1997.
49. **Van Herreweghe F, Mao J, Chaplen FW, Grooten J, Gevaert K, Vandekerckhove J, Vancompernolle K.** Tumor necrosis factor-induced modulation of glyoxalase I activities through phosphorylation by PKA results in cell death and is accompanied by the formation of a specific methylglyoxal-derived AGE. *Proc Natl Acad Sci USA* 99: 949–954, 2002.
50. **Wang Y, Zhou J, Minto AW, Hack BK, Alexander JJ, Haas M, Li YC, Heilig CW, Quigg RJ.** Altered vitamin D metabolism in type II diabetic mouse glomeruli may provide protection from diabetic nephropathy. *Kidney Int* 70: 882–891, 2006.
51. **Xu Y, Osborne BW, Stanton RC.** Diabetes causes inhibition of glucose-6-phosphate dehydrogenase via activation of protein kinase A, which contributes to oxidative stress in rat kidney cortex. *Am J Physiol Renal Physiol* 289: F1040–F1047, 2005.
52. **Yabe-Nishimura C, Nishinaka T, Iwata K, Seo HG.** Up-regulation of aldose reductase by the substrate, methylglyoxal. *Chem Biol Interact* 143–144: 317–323, 2003.
53. **Yoshida Y, Miyazaki K, Kamiie J, Sato M, Okuizumi S, Kenmochi A, Kamijo K, Nabetani T, Tsigita A, Xu B, Zhang Y, Yaoita E, Osawa T, Yamamoto T.** Two-dimensional electrophoretic profiling of normal human kidney glomerulus proteome and construction of an extensible markup language (XML)-based database. *Proteomics* 5: 1083–1096, 2005.